**Supplemental Information**

# Intracellular Ca$^{2+}$ Homeostasis and Nuclear

# Export Mediate Exit from Naive Pluripotency

Matthew S. MacDougall, Ryan Clarke, and Bradley J. Merrill

INVENTORY OF SUPPLMENTAL INFORMATION

Supplementary Figure Legends

Figure S1, Related to Figure 1
Figure S2, Related to Figure 1
Figure S3, Related to Figure 2
Figure S4, Related to Figure 3
Figure S5, Related to Figure 4
Figure S6, Related to Figure 5 and Figure 6
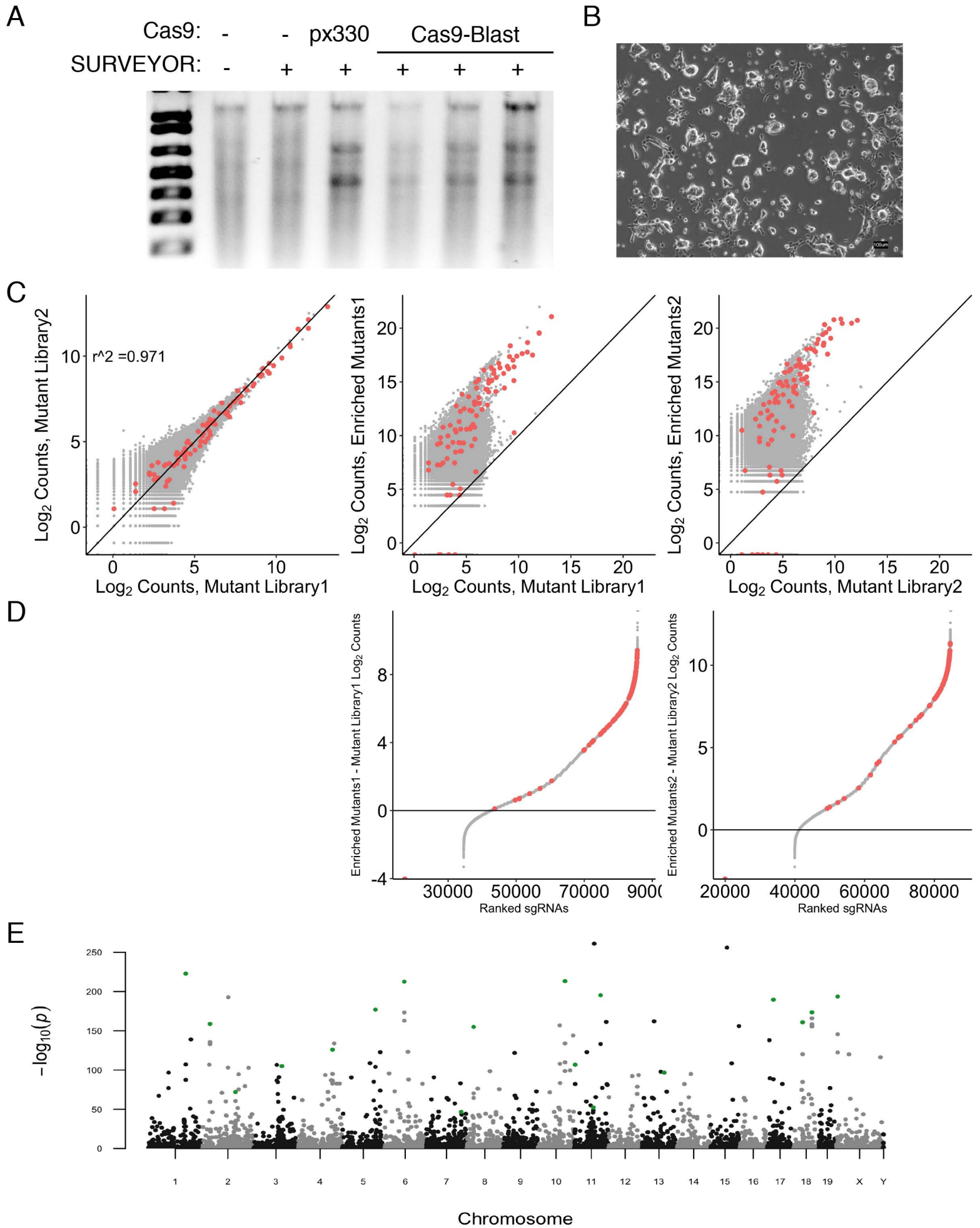
# Figure S1, Related to Figure1

A



B



C



D



E

**Figure S1, Related to Figure 1**
**A** Mismatch cleavage by SURVEYOR nuclease was used as a proxy measure of editing frequency in Cas9-Blast expression ESC transfected with pKLV-Lef1-PGKpuro-2a-tagBFP compared to wildtype ESC with transient expression of Cas9 and the same sgRNA. Related to Figure 2B.

**B** DIC Image displaying the morphology of stable, Cas9-Blast expressing ESC grown in 2iL on laminin and ornithine from **A.** Scale bar represents 100μm. Related to Figure 2B.

**C** Dotplots of sgRNA counts comparing mutant libraries to each other and to their selected pair. The red dots represent the sgRNAs associated with the top 25 genes identified in the screen. Related to Table S2 and Figure 2.

**D** Dotplots of the change in sgRNA count with replating selection. The red dots represent the sgRNAs associated with the top 25 genes identified in the screen. Related to Table S2 and Figure 2.
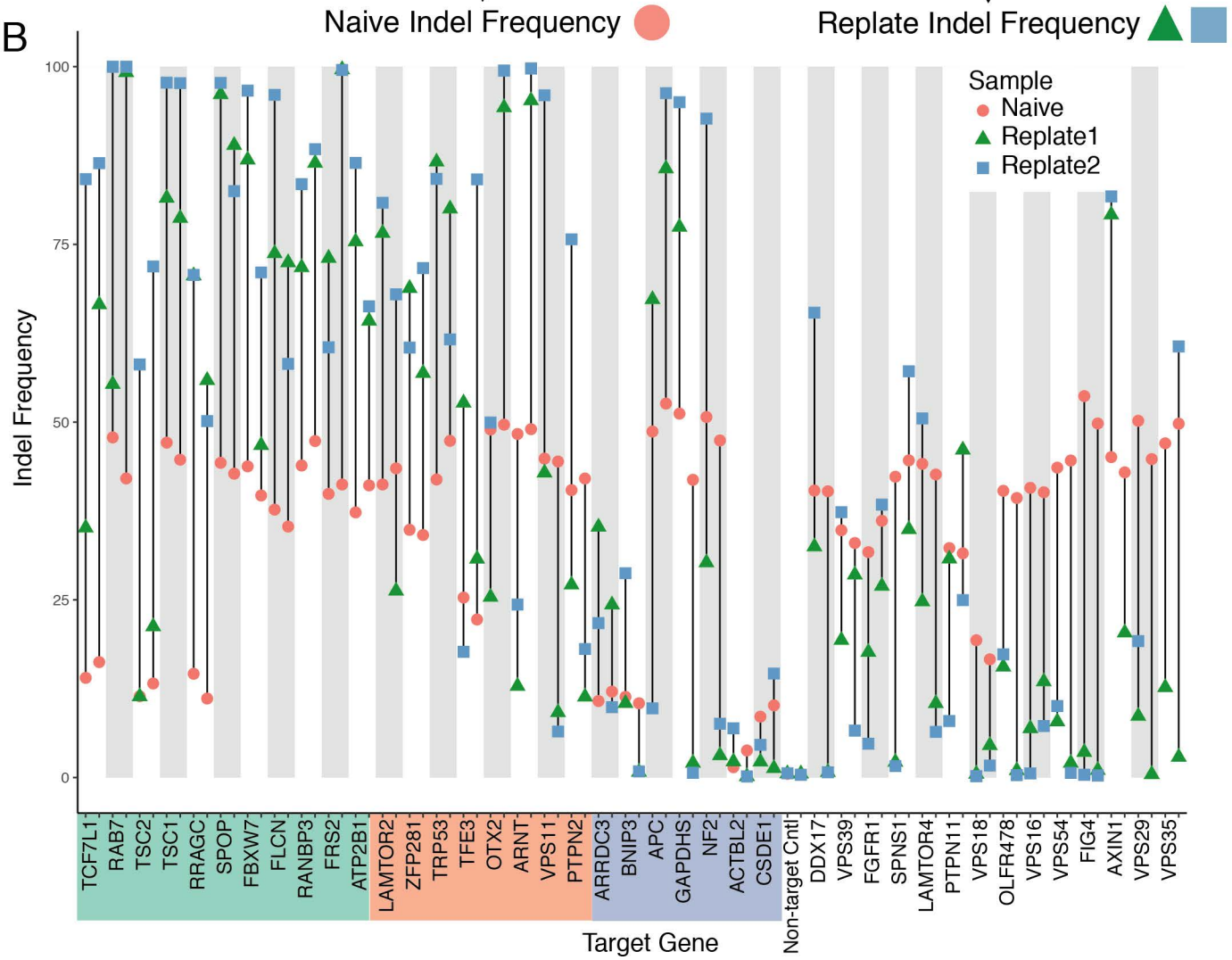
**E** Manhattan plot comparing genomic location of sgRNAs with the p-value of their enrichment calculated by the MAGeCK algorithm. The green dots represent the sgRNAs associated with the top 25 genes identified in the screen. Related to Table S2 and Figure 2.
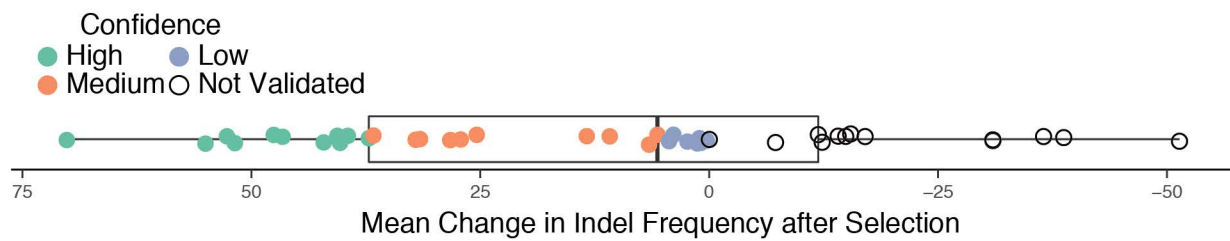
# Figure S2, Related to Figure 1
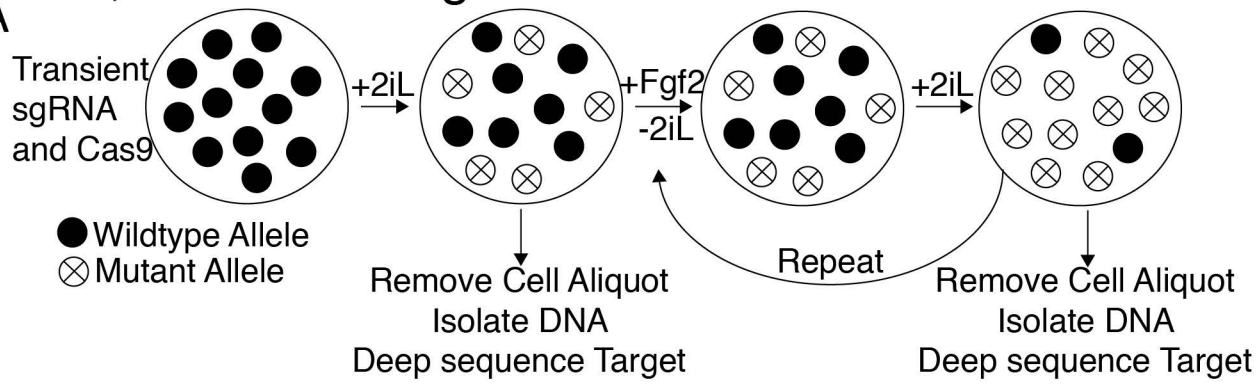
**Figure S2, Related to Figure 1**

**A** Arrayed validation takes advantage of heterogeneous gene editing outcomes from transient Cas9 and sgRNA expression to create a mixture of mutant and wildtype alleles at candidate, naïve exit genes. Two rounds of -2iL/+Fgf2-to-2iL replating is expected to positively select for gene disrupting mutant alleles for candidate genes that are required for naïve-exit. Cell aliquots are taken before and after each round of replating to measure mutant alleles as indel frequency by next-generation sequencing.

**B & C** The raw indel frequency (**B**) at candidate naïve-exit genes before and after selection is plotted. Experiments are performed in biological duplicate transfections (n=2) and the observations connected by a vertical line (**B**) are paired. **C** The mean change in indel frequency after selection, derived from **B,** is plotted as boxplot with overlaid swarmplot of all observations. Color coding indicates the confidence level of the validation and represents the mean change in indel frequency after selection for each naïve-exit candidate gene tested.
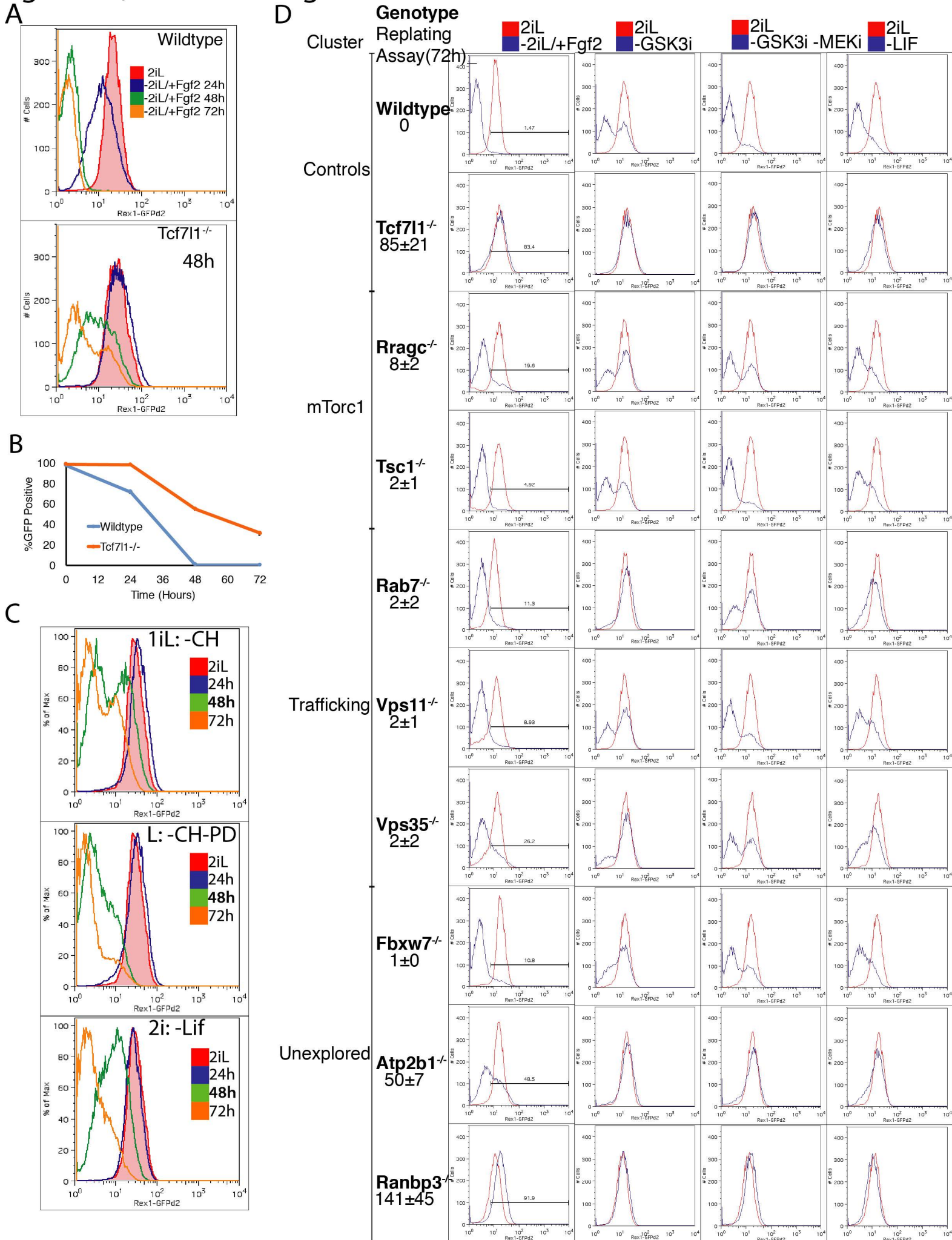
Figure S3, Related to Figure 2
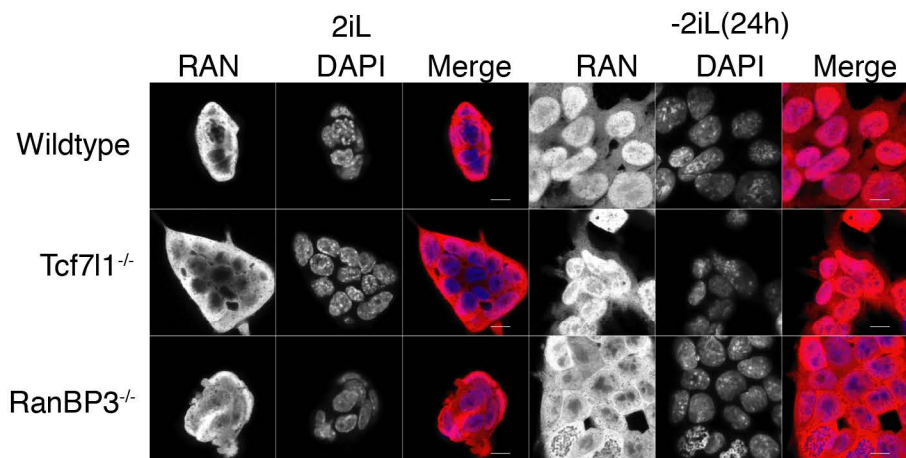
**Figure S3, Related to Figure 2**

**A & B** The fluorescence of naïve state reporter, Rex1-GFPd2, loss over time in -2iL/+Fgf2 for wildtype and Tcf7l1^{-/-} as flow histograms (**A**) and quantified as %GFP-positive (**B**).

**C** The Rex1-GFPd2 fluorescence sensitivity to withdrawal of the different 2iL components: -GSKi, -GSK3i/-MEKi, and -LIF. Withdrawal of the indicated component is followed over 72h.

**D** Raw, representative, Rex1-GFPd2 flow histograms for each mutant and treatment illustrated in Figure 3. These data are used to calculate the mean Rex1-GFPd2 fluorescence in Table S6. In addition, the mean colony counts ± standard deviation for each mutant (n=3) replated to 2iL after 72h of treatment with -2iL/+Fgf2 are shown below each genotype. Mutants are organized by assignment to the clusters illustrated to the left as in Figure 3.
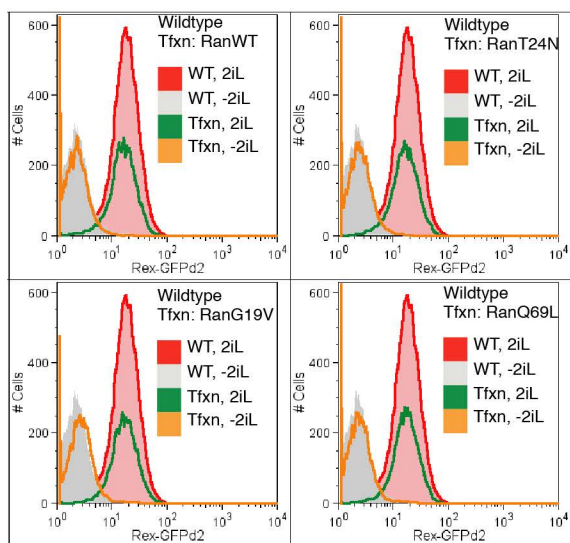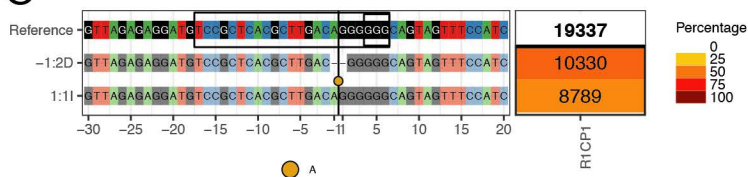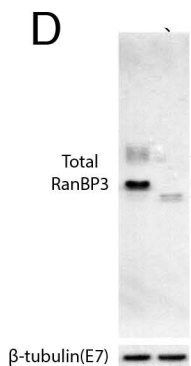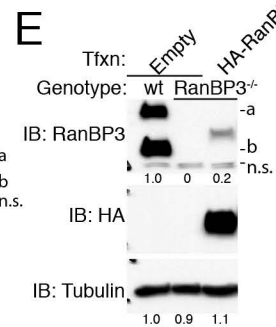
# Figure S4, Related to Figure 3
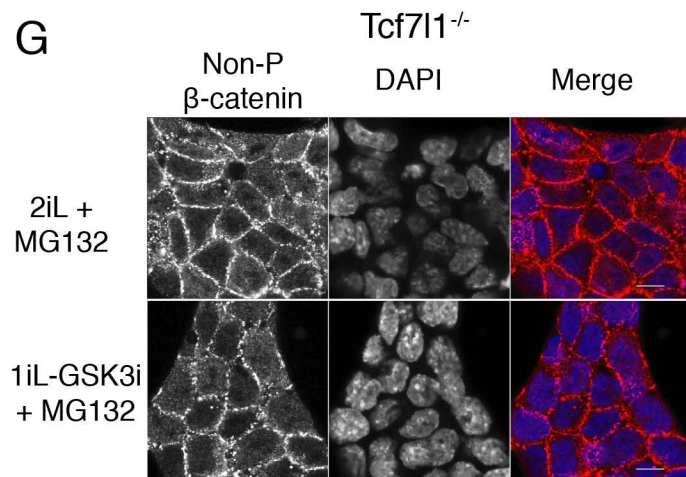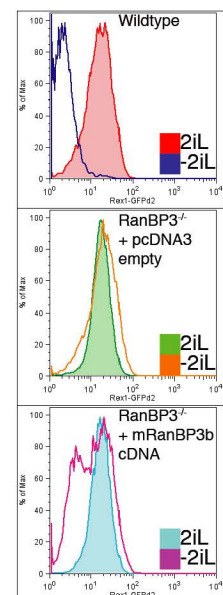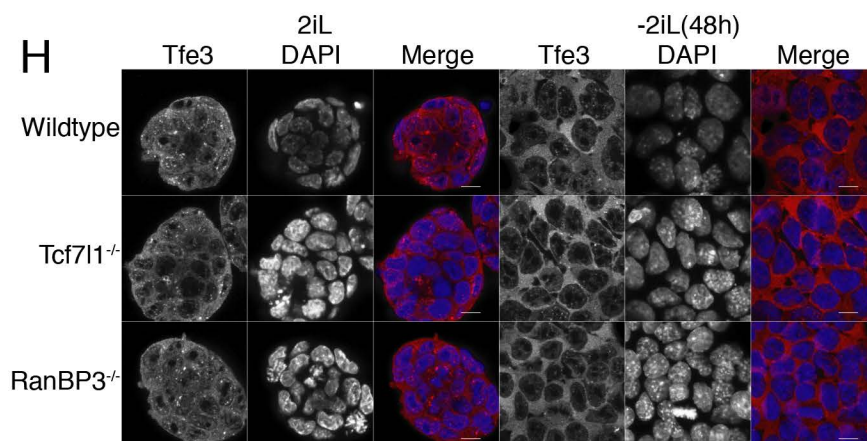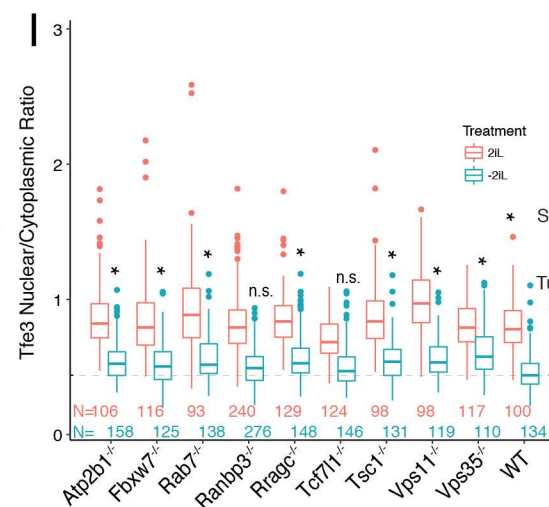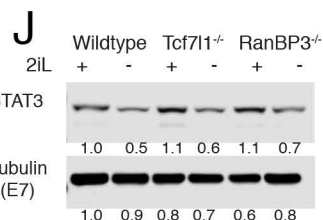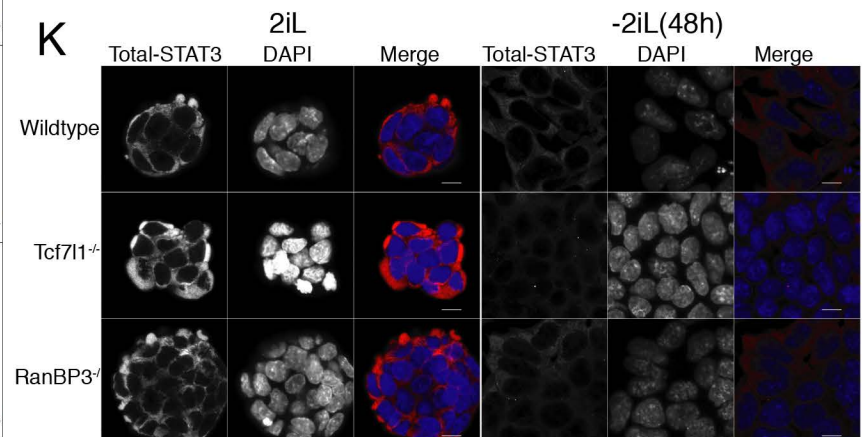
**Figure S4, Related to Figure 3**

**A** The cellular localization of Ran was determined by immunofluorescence in wildtype, Tcf7l1$^{-/-}$, and Ranbp3$^{-/-}$ cells in the presence or absence of 2iL for 24h. Representative images of n=3 experiments and >25 colonies. DAPI is used as a nuclear counterstain. Scale bar represents 10$\mu$m.

**B** Reporting the naïve state with Rex1-GFPd2 flow histograms of wildtype cells after 52h in the presence or absence of 2iL transiently transfected with RanWT-mCh, RanT24N-mCh, RanG19V-mCh, or RanQ69L-mCh. N=2 biological replicates of >10,000 live cell, singlet events were acquired for each treatment of each treatment.
Flow histograms of Rex1-GFPd2 are shown gated on mCh+, transfected cells. n=2 independent transfections.

**C** Next generation sequencing data showing the Ranbp3 reference sequence (top), sgRNA (boxed with PAM in second box), and alleles(below) present in the Ranbp3$^{-/-}$ cells used for functional characterization in Figure 4. The cut site is demarcated by the vertical line and the number of reads for each allele are shown to the right with shading representing frequency. Note: both alleles show a frameshift mutation.

**D** Western blot was used to confirm the absence of RanBP3 in Ranbp3$^{-/-}$ cells in 2iL with wildtype cells included as a control. beta-tubulin is used as a protein loading control. There are two known splice variants of Ranbp3, a and b, indicated as **-a** and **-b**. **n.s.** indicated a band that appears to be nonspecific to RanBP3.

**E & F** Mouse RanBP3 was transiently re-expressed in Ranbp3$^{-/-}$ cells and is detected by western blot for RanBP3 and HA-tag with beta-Tubulin shown as a protein loading control (**E**). Cells with this this transient re-expression were also subjected to flow cytometry to measure Rex1-GFPd2 fluorescence. Flow histograms of Rex1-GFPd2 are shown gated on mCherry-positive, transfected cells with expression of either empty vector or mRanBP3 in the presence or absence of 2iL (**F**). n=3 independent transfections.

**G** The localization of active, non-phosphorylated $\beta$-catenin was determined using immunofluorescence detection in Tcf7l1$^{-/-}$ cells in the presence or absence of GSK3i + MG-132 for 6h. Representative images of n=2 experiments and >10 colonies. DAPI is used as a nuclear counterstain. Scale bar represents 10$\mu$m. Yellow square regions are shown at right for detail with the nuclei indicated by the yellow arrowhead. Performed with Figure 3C.

**H** The cellular localization of Tfe3 was determined by immunofluorescence detection in wildtype, Tcf7l1$^{-/-}$, and Ranbp3$^{-/-}$ cells in the presence or absence of 2iL for 48h. Representative images of n=3 experiments and >15 colonies. DAPI is used as a nuclear counterstain. Scale bar represents 10$\mu$m.

**I** The experiment in **H** was performed for all candidate mutants and the nuclear Tfe3 immunofluorescence intensity (a.u.) of Tfe3 was quantified and plotted as a boxplot. Relevant statistical comparisons of marked genotype and treatment relative to wildtype -2iL are indicated by * (FDR < 5%) or n.s. (not significant).

**J** Western blot was used to detect total-Stat3 in wildtype, Tcf7l1$^{-/-}$, and Ranbp3$^{-/-}$ cells in the presence or absence of 2iL for 48h. Levels of beta-tubulin are measured as a loading control. n=1.

**K** The cellular localization of total-Stat3 was determined by **i**mmunofluorescence detection in wildtype, Tcf7l1$^{-/-}$, and Ranbp3$^{-/-}$ cells in the presence or absence of 2iL for 48h. Corresponds to Figure 4E as a control. Representative images of n=1 experiments and >5 colonies. DAPI is used as a nuclear counterstain. Scale bar represents 10μm.

Figure S5, Related to Figure 4

**Figure S5, Related to Figure 4**

**A** Next generation sequencing data showing the Atp2b1 reference sequence (top), sgRNA (boxed with PAM in second box), and alleles(below) present in the Atp2b1$^{-/-}$ cells used for functional characterization in Figure 5 and used to construct the Atp2b1$^{-/-}$Tcf7l1$^{-/-}$ double mutants in Figure 6. The cut site is demarcated by the vertical line and the number of reads for each allele are shown to the right with shading representing frequency. Note: both alleles show a frameshift mutation.

**B** Measurement of the Fura2 ratio for the indicated mutants in the <u>presence</u> of 2iL on gelatin for 48h. Ionomycin and BAPTA-AM treatments are used as controls for the assay. The horizontal line represents the mean Fura2 ratio for wildtype cells. The bars represent the mean Fura2 ratio ± standard deviation for n = 3.

**C** Measurement of the Fura2 ratio for the indicated mutants in the <u>absence</u> of 2iL on fibronectin for 48h. Ionomycin and BAPTA-AM treatments are used as controls for the assay. The horizontal line represents the mean Fura2 ratio for wildtype cells. The bars represent the mean Fura2 ratio ± standard deviation for n = 3.

**D** Control ionomycin and BAPTA-AM treatments for the time course shown in Figure 4A before and after 2iL withdrawal for 48h. The dotted horizontal line represents the mean Fura2 ratio for wildtype cells grown in 2iL. The bars represent the mean Fura2 ratio ± standard deviation for n = 3 except for the ionomycin treatments which are n=1.

**E** Empirical measurement of Fura2 ratio after treating wildtype ESC with different calcium modulators: Sea0400 (NCXi), Calcitonin (CT), and Carboxyeosin (Carbox). Atp2b1$^{-/-}$ treatment is used as a control. The bars represent the mean Fura2 ratio ± standard deviation for n = 3. The horizontal line represents the mean Fura2 ratio for wildtype cells grown in 2iL. * and # represent an FDR < 5% and <10% compared to wildtype, respectively.

**F** Reporting the naïve state with Rex1-GFPd2 flow histograms of wildtype cells after 52h in the presence or absence of 2iL with or without Calcitonin (100nM). N=2 biological replicates of >10,000 live cell, singlet events were acquired for each treatment of each treatment.

**G** DIC images displaying the morphology of ESC grown in presence or absence of 2iL with or without NCXi. Scale bar represents 200μm.

**H** The mean colony counts ± standard deviation for wildtype and Atp2b1$^{-/-}$ cells replated to 2iL after 72h of treatment in the presence or absence of 2iL with or without NCXi. N=3 biological replicates.

**I** DIC images displaying the morphology and density of wildtype ESC grown in 2iL or GSK3i + CsA for indicated lengths of time. Scale bar represents 200μm.

**J** Reporting the naïve state with Rex1-GFPd2 flow histograms of wildtype, Atp2b1$^{-/-}$, Tcf7l1$^{-/-}$ cells after 40h (top row) or 48h (bottom row) in the presence or absence of 2iL and/or Calcineurin/NFAT inhibitors (cyclosporin A (CsA), FK506, VIVIT) to reduce the signaling effects of intracellular calcium. N=2 biological replicates of >10,000 live cell, singlet events were acquired for each treatment of each mutant/treatment.

**K & L** Schematic of the targeting mCh to the mAtp2b1 locus with CRISPR mediated homology directed repair. Genotyping primers to confirm correct location of insertion **(K)**. The genotyping PCRs to confirm correct Atp2b1-mCh insertion are shown in **L.** Related to Figure 4D.

**M** Intracellular free calcium and ER calcium is visualized in wildtype or Atp2b1$^{-/-}$ cells transfected with the genetically encoded calcium indicators, GCaMP5G and R-CEPIAer. Transfected cells are treated in the presence or absence of 2iL for 24h prior to live-cell imaging. Scale bar represents 10$\mu$m.

Figure S6, Related to Figures 5 and 6

**Figure S6, Related to Figure 5 and Figure 6**

**A** DIC images displaying the morphology and density of wildtype, Tcf7l1$^{-/-}$, Ranbp3$^{-/-}$, and Atp2b1$^{-/-}$ ESC grown in N2B27 for indicated lengths of time. Scale bar represents 200$\mu$m.

**B** Next generation sequencing data showing the Tcf7l1 alleles present in the Atp2b1$^{-/-}$ cells during generation of Atp2b1$^{-/-}$ Tcf7l1$^{-/-}$ double mutant ESC. The frequency of each allele and the raw read counts are shown to the right.

**C** The mean colony counts ± standard deviation for wildtype, single, and double Atp2b1$^{-/-}$ Tcf7l1$^{-/-}$ mutant cells replated to 2iL after indicated passages in N2B27. **Left:** Replate after first passage; raw colony count. **Right:** Replating after the indicated passage number relative to Tcf7l1 colony count. N=2 biological replicates.

**D** High magnification immunofluorescence for Nanog in inhibitor independent, Atp2b1$^{-/-}$ Tcf7l1$^{-/-}$ double mutant cells maintained in N2B27. Images are acquired from experiment shown in Figure 6E. The arrow shows an exemplar Nanog+ nucleus and the arrowhead shows an exemplar Nanog- nucleus within the same colony. Scale bar represents 10$\mu$m.

**E** The presence and localization of Sox2 was determined by immunofluorescence detection in wildtype, Tcf7l1$^{-/-}$, Atp2b1$^{-/-}$, double Atp2b1$^{-/-}$ Tcf7l1$^{-/-}$ mutant cells in 2iL as well as inhibitor independent, Atp2b1$^{-/-}$ Tcf7l1$^{-/-}$ double mutant cells maintained in N2B27. Cells are grown on gelatin. Representative images of n=2 experiments and >25 colonies. DAPI is used as a nuclear counterstain. Scale bar represents 10$\mu$m.

**F** DIC images displaying the morphology and density of wildtype ESC grown in combinations of GSK3i or MEKi with different calcium modulators: Sea0400 (NCXi), Calcitonin (CT), and Carboxyeosin (Carbox) for indicated lengths of time. Scale bar represents 200$\mu$m.

**G** DIC images displaying the morphology and density of Tcf7l1$^{-/-}$ and Atp2b1$^{-/-}$ ESC grown in GSK3i, CT, or CTCH for indicated lengths of time. Scale bar represents 200$\mu$m.

**H** Live cell proliferation of wildtype, Tcf7l1$^{-/-}$, Atp2b1$^{-/-}$, Atp2b1$^{-/-}$ Tcf7l1$^{-/-}$ double mutant ESC maintained in indicated media (2iL, N2B27 or CTCH) through 72h measured by subtracting the propidium iodide positive cells from the Hoechst 33342 positive cells.

**I** Embryoid bodies were formed for 5-9 days from ESC cultured in either 2iL or CTCH for more than five passages. The presence and localization of the indicated pluripotency, mesodermal, endodermal, and ectodermal markers were determined by immunofluorescence detection using antibodies specific for the antigen indicated on each image or Hoechst 33342 staining for DNA. Representative images of more than 15 embryoid bodies for each marker are shown. Embryoid bodies at day 9 were used for FoxA2, Sox1, Nestin, and βIII-tubulin, day 7 were used for Nanog, Eomes, and CK19, and day 5 for Nanog. Scale bar represents 15$\mu$m.